A Study on the Tensile Behavior of Specimens Manufactured by FDM from Recycled PETG in the Context of the Circular Economy Transition

Dragos Gabriel Zisopol
Mechanical Engineering Department, Petroleum - Gas University Ploiesti, Romania
zisopold@upg-ploiesti.ro

Mihail Minescu
Mechanical Engineering Department, Petroleum - Gas University Ploiesti, Romania
mminescu@upg-ploiesti.ro

Dragos Valentin Iacob
Department of Mechanical Engineering, Doctoral School, Petroleum - Gas University, Ploiesti, Romania
dragoshicb@gmail.com (corresponding author)

Received: 5 September 2024 | Revised: 3 October 2024 and 22 October 2024 | Accepted: 26 October 2024

 DOI: https://doi.org/10.48084/etasr.8927

ABSTRACT

This article presents the results of a study on the influence of 3D printing by Fused Deposition Modeling (FDM) parameters on the tensile behavior of parts made from Everfil recycled Polyethylene Terephthalate Glycol (rPETG). For this study, 27 rPETG tensile specimens with 100% recycled material were manufactured using an Anycubic 4 Max Pro 2.0 3D printer and by varying the printing parameters: height of the deposited layer in one pass, L_h, and filling percentage, I_d. The L_h was set to 0.10, 0.15, and 0.20 mm and the I_d was set to 50, 75, and 100 %. The two variable parameters, I_d and L_h, influenced the tensile characteristics of the rPETG specimens: maximum breaking strength, percent elongation at break, and modulus of elasticity. The ultimate breaking strength and modulus of elasticity of the rPETG specimens were most influenced by I_d, whereas the percentage elongation at break was mostly affected by L_h. The optimized FDM parameters for the fabrication of rPETG tensile specimens were found to be L_h = 0.20 mm and I_d = 100%.

Keywords-FDM parameters; rPETG; tensile strength; percent elongation; modulus of elasticity; circular economy

I. INTRODUCTION

Plastic materials have many advantages over the metallic materials, with one of the most important being their lower production cost [1-5]. This major advantage has led to a massive increase in plastic demand, which has given rise to a global problem: plastic waste and the reduced lifecycle of materials used for packaging [6-9]. At a European Union level, it is desirable for a completely circular economy to have been reached by 2050 [10, 11]. The circular economy is a production and consumption concept associated with sustainable development and refers to increasing material lifetime by deploying the 3R concept (Recovery, Recycling, Reuse) in the creation of new products [12, 13]. Additive manufacturing technologies have led to the sustainable development and circular economy concepts because, unlike conventional manufacturing technologies, namely formative and subtractive, parts are made by adding material in overlapping layers using additive manufacturing technologies, while the amount of technological waste is negligible [14-19]. Additive manufacturing technologies have been continuously evolving since their inception, and through this evolution, faster, more precise, and accessible equipment, a diverse range of materials, as well as better-performing CAD and slicer software have emerged [20-22]. In the context of the transitioning to a circular economy in the field of additive manufacturing technologies through the extrusion of thermoplastics, plastic materials are manufactured from virgin plastic material granules and recycled plastic material granules [1-3, 14]. There is a wide assortment of plastic materials suitable for additive manufacturing technologies by extrusion of thermoplastics that contain recycled material in their composition, that is, recycled Polyethylene Terephthalate (rPET), recycled Polyethylene Terephthalate Glycol (rPETG), recycled Acrylonitrile Styrene Acrylate (rASA), recycled Polylactic Acid (rPLA), and others [1-3, 20, 21].

In [23], the impact of printing parameters on the tensile behavior of specimens made from rPET and rPETG using Fused Granular Fabrication (FGF) manufacturing was investigated. The parameters that were varied for the tensile specimens were the layer height deposited in one pass, L_h, the percentage filling density, I_d, and the number of contours, N_c. The maximum breaking strength of 26.4 ± 1.2 MPa was observed for rPET specimens manufactured with the parameters L_h = 1.1 mm, I_d = 70%, and N_c = 3. However, for the tensile specimens manufactured from rPETG, the highest value of breaking strength of 44.8 ± 6.6 MPa was recorded for the group of samples manufactured with parameters L_h = 1.2 mm, I_d = 100%, and N_c = 2. In [24], the tensile behavior of specimens manufactured using Fused Deposition Modeling (FDM) and recycled PETG was investigated. The specimens that were manufactured and tested consisted of 100% PETG, 50% granulated PETG and 50% rPETG, 100% rPETG, 100% rPETG pelletized, and Verbatim brand PETG. The highest breaking strength was obtained for the sample with 100% PETG, exhibiting a 10% higher breaking strength than the sample made of the Verbatim filament. The breaking strength of the 100% rPETG sample was 13% lower than that of the specimen made of Verbatim brand filament. In [25], Analysis of Variance (ANOVA) was employed to determine the optimized FDM printing parameters of the rPET samples. rPET Ultrafuse® and rPET filaments were used to manufacture tensile specimens, and four parameters were varied: extruder temperature, T_e, height of the deposited layer in one pass, L_h, filling density, I_d, and printing speed, P_s. The results of the study showed that from the 4 parameters studied, the L_h had a significant influence on the breaking resistance of the rPET specimens. Moreover, it was demonstrated that by increasing the height of the layer deposited at one pass, higher values of the resistance to break can be achieved.

The novelty of this work lies in the determination of the influence of the FDM parameters, L_h (the height of the layer deposited in one pass), and I_d (the filling density) on the tensile behavior of parts made from rPETG in the context of the transition to a circular economy. Simultaneously, an optimization of the FDM parameters was carried out to maximize the values of the tensile characteristics of the rPETG samples.

The samples were produced and tested in the laboratories of the Faculty of Mechanical and Electrical Engineering of the Petroleum – Gas University of Ploiești.

II. WORK METHODOLOGY

Figure 1 displays the stages of the work methodology regarding the influence of the FDM parameters on the tensile behavior of the rPETG parts.

SolidWorks 2023 software [26] was utilized to create the 2D (Figure 2a) and the 3D models (Figure 2b) of the tensile specimens. The 3D model of the sample was converted from SLD format to STL format (Figure 2c) [20-22].

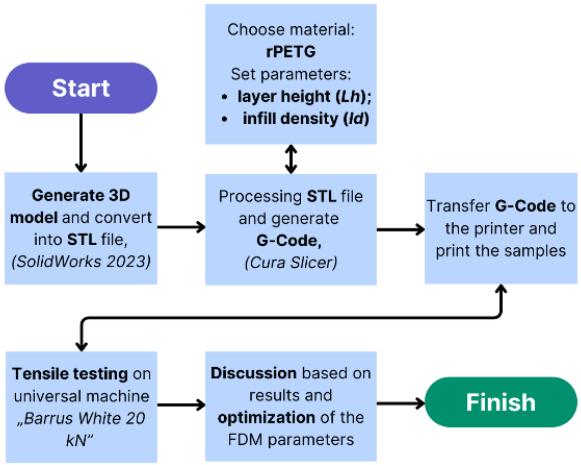

Fig. 1. The stages of the working methodology regarding the research of the influence of FDM parameters on the tensile behavior of rPETG parts.

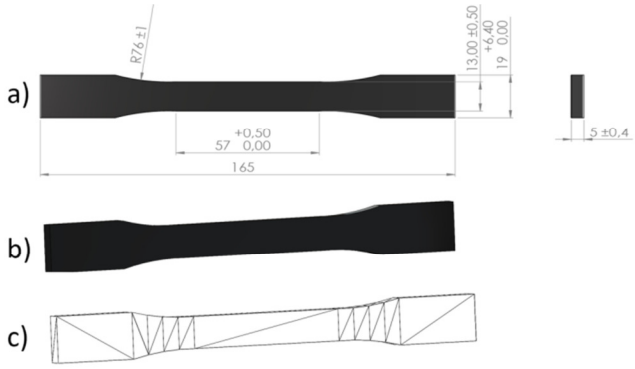

Fig. 2. Tensile test specimen in SolidWorks 2023: (a) 2D model, (b) 3D model, (c) STL model.

Using the STL format file corresponding to the tensile specimen exhibited in Figure 2c and the FDM printing parameters evidenced in Table I, a G-Code file for the fabrication of the tensile specimens was generated using Cura Slicer software (version 5.7.2) [27].

The G-Code file was transferred to the Anycubic 4 Max Pro 2.0 3D printer [28], illustrated in Figure 3. 27 tensile specimens, observed in Figure 4, were fabricated using an rPETG filament of 1.75 mm diameter supplied from Everfill.

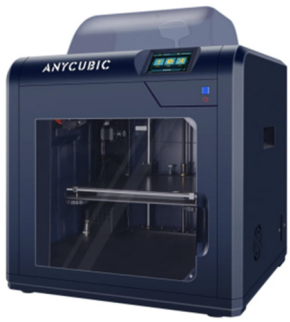

Fig. 3. The 3D printer Anycubic 4 Max Pro 2.0, which was used to manufacture the tensile specimens from ASA through FDM.

TABLE I. FDM PRINTING PARAMETERS FOR 3D PRINTING TENSILE SAMPLES.

Constant parameters		Variable parameters		Material
		Layer height	Infill density	rPETG
		L_h (mm)	I_d (%)	(pieces)
Part orientation, Po	X-Y	0.10	100	3
Temperature of the extruder, Et (°C)	250		75	3
			50	3
Temperature of the platform, Bt (°C)	70	0.15	100	3
			75	3
Printing speed, Ps (mm/s)	30		50	3
		0.20	100	3
Infill pattern, Ip	Grid		75	3
			50	3

Fig. 4. The rPETG tensile test specimens were fabricated via FDM using an Anycubic 4 Max Pro 2.0 3D printer.

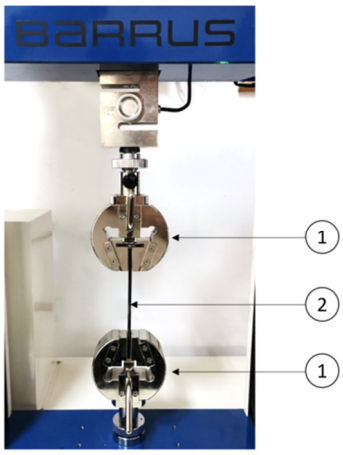

Fig. 5. Tensile test on universal testing machine "Barrus White 20 kN": 1 – grips; 2 – tensile sample.

The tensile specimens portrayed in Figure 4 were fabricated by FDM on the Anycubic 4 Max Pro 2.0 printer using the parameters evidenced in Table I and were tensile tested on the "Barrus White 20 kN" universal testing apparatus manifested in Figure 5, according to the ASTM standard D638-14, at a speed of 5 mm/min [29].

III. RESULTS AND DISCUSSION

Figure 6 shows the 27 rPETG specimens after the tensile test.

Fig. 6. The rPETG specimens after the tensile test.

A. *Influence of FDM Parameters on the Tensile Strength of rPETG Tensile Specimens*

The results from the tensile strength experiments of the tensile specimens fabricated by FDM from rPETG are plotted in Figures 7 – 9 for L_h values of 0.10, 0.15, and 0.20 mm.

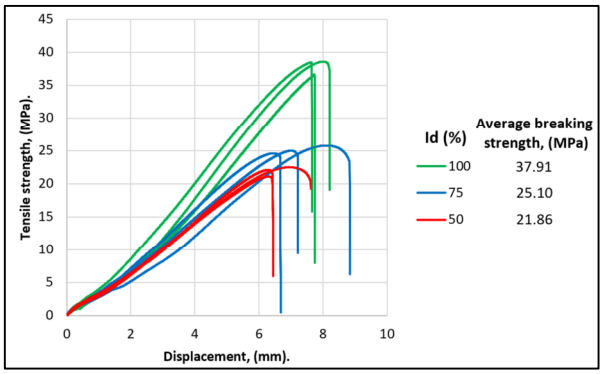

Fig. 7. Average values of breaking strength of rPETG specimens with L_h = 0.10 mm and I_d = 50, 75, and 100 %.

Analyzing Figure 7, it is observed how the filling percentage influences the breaking resistance of the rPETG samples. The highest breaking strength values of 36.64 – 38.58 MPa were obtained for the samples with 100% filling percentage. By increasing the filling percentage from 50% to 75%, the breaking tensile strength increased by 12.76 – 14.36%, and by increasing the filling percentage from 75% to 100%, the breaking strength increased by 32.88 – 33.24%. Figure 8 demonstrates that the I_d parameter had a significant influence on the breaking strength of the samples made of rPETG, with an L_h of 0.15 mm. The highest values were obtained for the samples with a filling of 100% (25.17 – 26.71 MPa). By increasing the filling percentage from 50% to 75%, the tensile strength increased by 8.50%, and by increasing the filling percentage from 75% to 100%, the tensile strength increased by up to 2.63%.

From Figure 9, it can be observed that for the samples with L_h of 0.20 mm the filling percentage decisively influences the resistance of the rPETG samples to tearing. The highest breaking strength values ranged between 40.98 and 41.55 MPa for the samples with a 100% filling percentage. By increasing the filling percentage from 50% to 75%, the breaking tensile strength increased by 22.58 - 24.84%, and by increasing the filling percentage from 75% to 100%, the breaking strength increased by up to 29.16%.

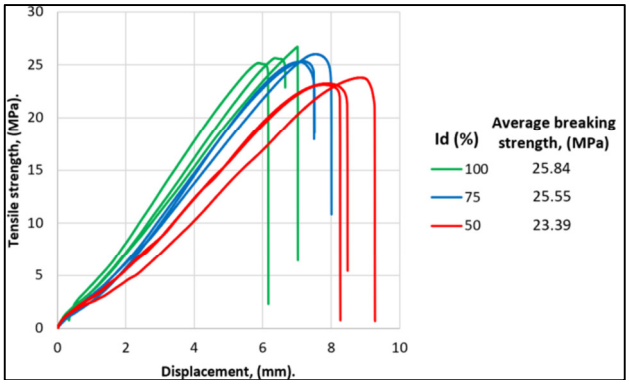

Fig. 8. Average values of breaking strength of rPETG specimens with L_h = 0.15 mm and I_d = 50/75/100 %.

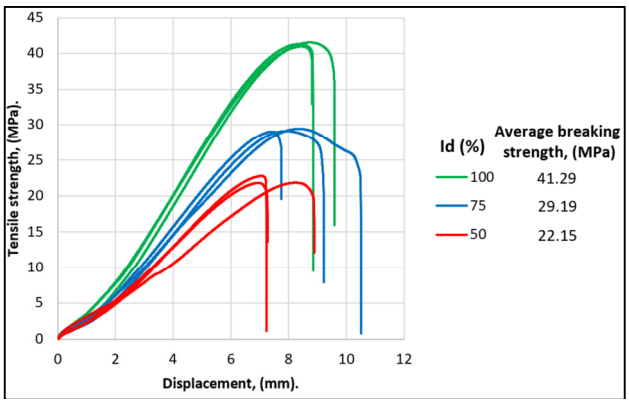

Fig. 9. Average values of breaking strength of rPETG specimens with L_h = 0.20 mm and I_d = 50/75/100 %.

Using the Minitab software [30], the Pareto chart evidenced in Figure 10 was plotted, which compares the standardized effects of the two varied parameters, L_h and I_d, on fracture toughness.

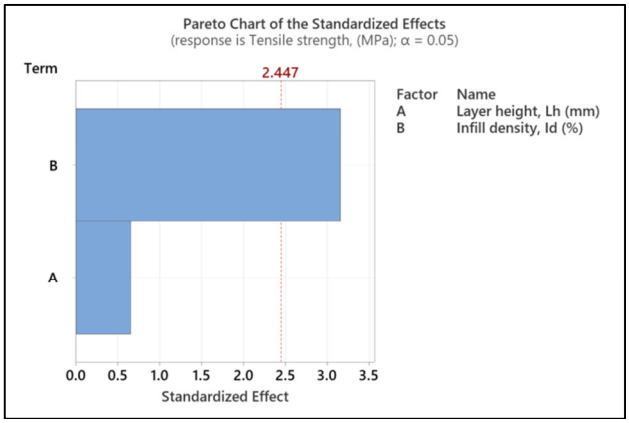

Fig. 10. Pareto chart showing the influence of L_h and I_d on breaking strength.

According to the Pareto graph in Figure 10, the percentage of filling decisively influences the resistance to breaking of the samples made by FDM from rPETG.

In Figure 11, the contour graph of the tensile strength for L_h was drawn between 0.10 – 0.20 mm, and I_d varied between 50 - 100% using Minitab [30].

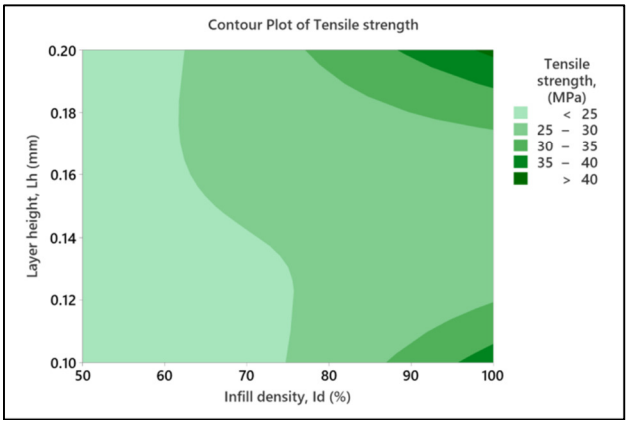

Fig. 11. Contour plot of breaking strength.

The contour plot illustrated in Figure 11 shows that higher breaking strength values can be obtained with higher filling percentages. Moreover, the influence of L_h on tensile strength was marginal.

B. Influence of FDM Parameters on the Percentage Elongation at Break of rPETG Tensile Specimens

Figure 12 displays the percentage elongation at break for L_h values of 0.10, 0.15, and 0.20 mm, and I_d of 50, 75, and 100%.

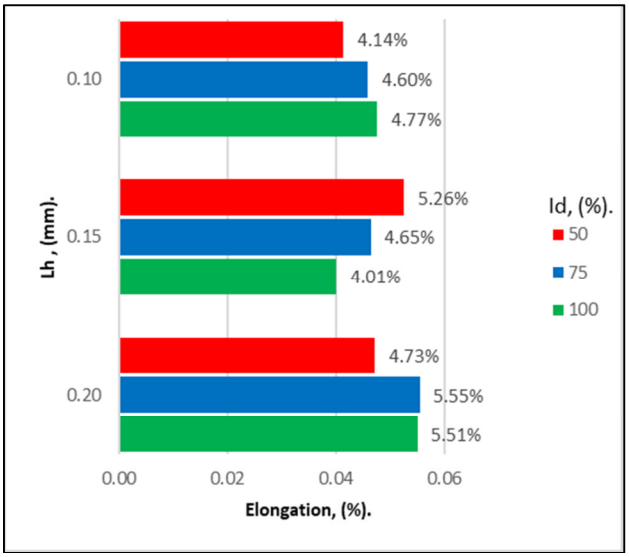

Fig. 12. The average values of the percentage elongation at break of the rPETG samples.

According to Figure 12, the percentage of elongation at break was influenced by the filling percentage. The highest elongation of 5.59 - 6.37% was recorded for samples with a filling percentage of 75%. With an increase in the filling percentage from 50% to 75%, the elongation at break increased

by 11.04 – 17.46%. By increasing the filling percentage from 75 to 100%, the elongation at break increased by up to 3.81%.

Figure 13 depicts the Pareto chart comparing the standardized effects of the two varied parameters, L_h and I_d, on the percentage elongation at break.

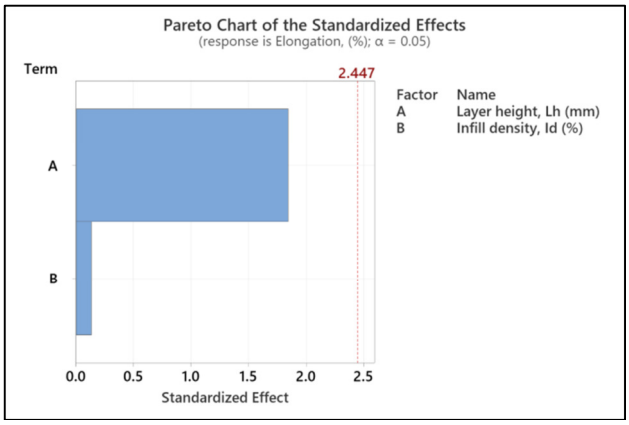

Fig. 13. Pareto chart with the influence of L_h and I_d on the percentage elongation at break of the rPETG samples.

The Pareto chart in Figure 13 shows that out of the two factors, L_h and I_d, L_h has a greater influence on the percentage elongation at break of the rPETG specimens. The contour graph of the percentage of elongation at break is demonstrated in Figure 14.

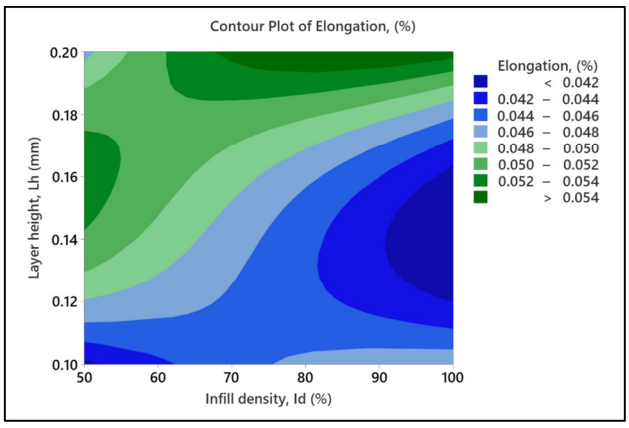

Fig. 14. Contour plot of percentage elongation at break.

It can be concluded from Figure 14 that higher values of layer height in one pass result in an extended elongation at break. This observation is more prominent to lower filling percentages.

C. *Influence of FDM Parameters on the Modulus of Elasticity at Break of rPETG Tensile Specimens*

Figure 15 presents the average values of the modulus of elasticity for L_h values of 0.10, 0.15, and 0.20 mm, and I_d of 50, 75, and 100%.

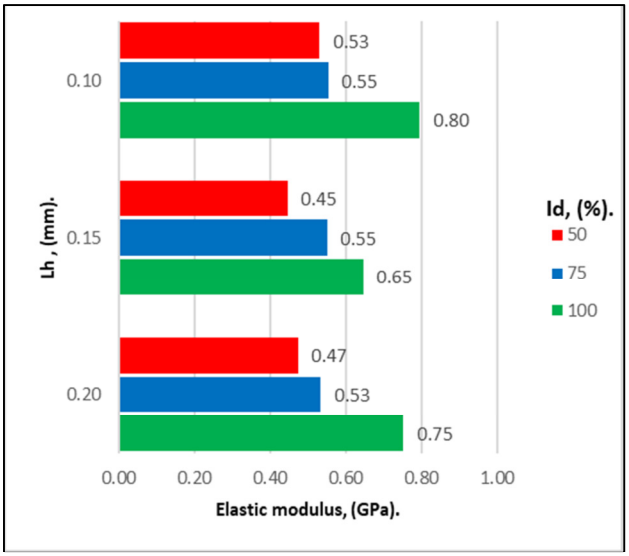

Fig. 15. Average values of the modulus of elasticity of the rPETG samples.

From Figure 15, it can be observed that the modulus of elasticity is influenced by the FDM parameters. The highest values of the modulus of elasticity were obtained for the samples with L_h parameters of 0.10 mm and I_d of 100%. When the percentage of filling increased from 50% to 75%, the modulus of elasticity increased by 4.12 - 23.28%, and when the percentage of filling increased from 75% to 100%, the modulus of elasticity increased by 17.45 - 43.88%. When the height of the deposited layer decreased from 0.20 to 0.15 mm, the modulus of elasticity decreased by 5.84 – 14.04%, and when L_h decreased from 0.15 mm to 0.10 mm, the modulus of elasticity increased by 19.09 – 23.22%.

Figure 16 illustrates the Pareto chart of the standardized effects of the two varied parameters, L_h and I_d, on the modulus of elasticity.

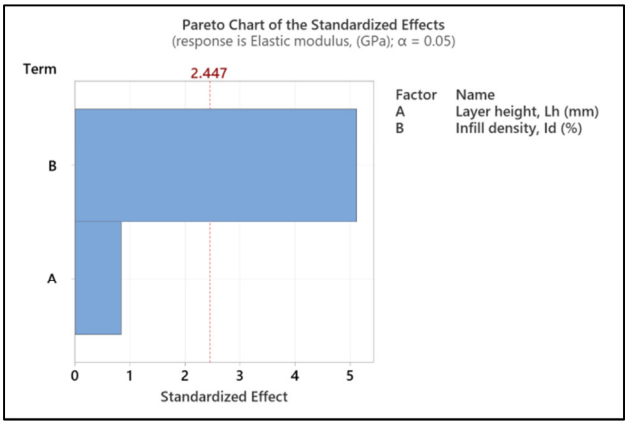

Fig. 16. Pareto chart showing the influence of L_h and I_d on the modulus of elasticity.

The Pareto chart exhibited in Figure 16 clearly demonstrates that the filling percentage has a greater influence

on the modulus of elasticity than the layer height deposited in one pass.

Figure 17 shows a contour graph of the modulus of elasticity for L_h and I_d values ranging between 0.10 and 0.20 mm and 50-100%, respectively.

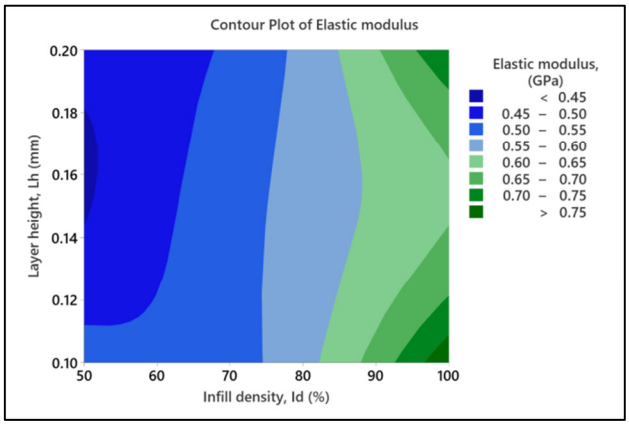

Fig. 17. Contour plot of the elastic modulus.

The diagram in Figure 17 indicates that the modulus of elasticity increased with an increase in the filling percentage.

As observed in Figure 18, the FDM parameters were optimized to maximize the tensile characteristics, namely tear strength, percentage elongation at break, and modulus of elasticity, of the samples made of rPETG.

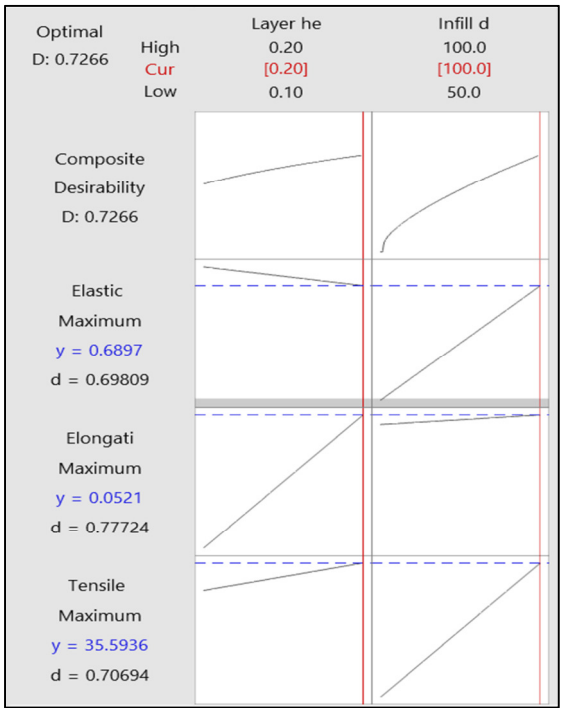

Fig. 18. Optimization plot of FDM parameters (L_h and I_d) for maximizing tensile characteristics of rPETG specimens.

According to Figure 18, the optimal FDM parameters for maximizing the tensile characteristics of the samples made of rPETG are L_h = 0.20 mm and I_d = 100%.

IV. CONCLUSIONS

This paper presents research results regarding the influence of Fused Deposition Modeling (FDM) parameters, such as the height of the layer deposited in one pass, L_h, and filling density, I_d, on the tensile behavior of specimens made of recycled Polyethylene Terephthalate Glycol (rPETG). Using the Anycubic 4 Max Pro 2.0 3D printer, 27 rPETG specimens were made with 100% Everfil recycled material using the parameters listed in Table I. All 27 specimens were tensile tested on the universal testing machine "Barrus White 20 kN ".

The minimum average tensile strength of 21.86 MPa was recorded for specimens made by rPETG and FDM, with the parameters L_h set at 0.10 mm and I_d at 50%. The maximum average tensile strength of 41.29 MPa was recorded for the set of samples with parameters L_h of 0.20 mm and I_d of 100%. The minimum average percentage elongation at break of 4.01% was recorded for the set of samples with parameters L_h of 0.15 mm and I_d 100%. The parameters L_h of 0.20 mm and I_d of 75% gave the samples with the maximum average percentage elongation at break of 5.55%. The minimum modulus of elasticity of 0.45 GPa was recorded for the set of specimens with the parameters L_h of 0.15 mm and I_d of 50%. The maximum modulus of elasticity of 0.80 GPa was recorded for the set of specimens with the parameters L_h of 0.10 mm and I_d of 100%.

Comparing this study's results with the literature, it is observed that the resistance to breaking of the proposed rPETG samples is higher by 29.17 – 31.59% compared to other PETG samples [14].

Using the Minitab software, a statistical analysis of the influence of the FDM parameters on the tensile behavior of the samples made of rPETG was performed. The filling percentage significantly influenced the breaking strength and modulus of elasticity. However, the layer height deposited at one pass had a greater impact on the percentage elongation at break than I_d. In order to maximize the values of the traction characteristics, by utilizing the Minitab software the FDM parameters were optimized, and the optimal values were found to be L_h = 0.20 mm and I_d = 100%.

The results of the study certify that the use of recycled materials in applications of additive manufacturing technologies through thermoplastic extrusion represents a viable solution for plastic waste management. The conclusions of this study can be extrapolated to FDM printing using other recycled materials with different percentages of recycled material.

V. REFERENCES

[1] A. Oussai, Z. Bártfai, and L. Kátai, "Development of 3D Printing Raw Materials from Plastic Waste. A Case Study on Recycled Polyethylene Terephthalate," *Applied Sciences*, vol. 11, no. 16, Jan. 2021, Art. no. 7338, https://doi.org/10.3390/app11167338.

[2] M. Jürgens and H.-J. Endres, "Environmental impacts of circular economy practices for plastic products in Europe: Learnings from life

cycle assessment studies," *Procedia CIRP*, vol. 122, pp. 312–317, Jan. 2024, https://doi.org/10.1016/j.procir.2024.01.046.

[3] I. Pfisterer, R. Rinberg, L. Kroll, and N. Modler, "Quality-Driven Allocation Method to Promote the Circular Economy for Plastic Components in the Automotive Industry," *Recycling*, vol. 9, no. 4, Aug. 2024, Art. no. 67, https://doi.org/10.3390/recycling9040067.

[4] E. R. Larson, "An Overview of Thermoplastic Materials," in *Thermoplastic Material Selection*, vol. 4, William Andrew Publishing, 2015, pp. 97–143.

[5] M. Ciornei, R. I. Iacobici, I. D. Savu, and D. Simion, "FDM 3D Printing Process - Risks and Environmental Aspects," *Key Engineering Materials*, vol. 890, pp. 152–156, 2021, https://doi.org/10.4028/www.scientific.net/KEM.890.152.

[6] P. K. Dey, C. Malesios, S. Chowdhury, K. Saha, P. Budhwar, and D. De, "Adoption of circular economy practices in small and medium-sized enterprises: Evidence from Europe," *International Journal of Production Economics*, vol. 248, Jun. 2022, Art. no. 108496, https://doi.org/10.1016/j.ijpe.2022.108496.

[7] B. D. Hettiarachchi, J. I. Sudusinghe, S. Seuring, and M. Brandenburg, "Challenges and Opportunities for Implementing Additive Manufacturing Supply Chains in Circular Economy," *IFAC-PapersOnLine*, vol. 55, no. 10, pp. 1153–1158, Jan. 2022, https://doi.org/10.1016/j.ifacol.2022.09.545.

[8] S.-V. Galaţanu *et al.*, "Mechanical behavior of recycled FDM printed parts from PETG in the circular economy," *Procedia Structural Integrity*, vol. 56, pp. 138–143, Jan. 2024, https://doi.org/10.1016/j.prostr.2024.02.048.

[9] N. Vidakis *et al.*, "Sustainable Additive Manufacturing: Mechanical Response of Polyethylene Terephthalate Glycol over Multiple Recycling Processes," *Materials*, vol. 14, no. 5, Jan. 2021, Art. no. 1162, https://doi.org/10.3390/ma14051162.

[10] M. Agovino, M. Cerciello, G. Musella, and A. Garofalo, "European waste management regulations and the transition towards circular economy. A shift-and-share analysis," *Journal of Environmental Management*, vol. 354, Mar. 2024, Art. no. 120423, https://doi.org/10.1016/j.jenvman.2024.120423.

[11] European Parliament, "How the EU wants to achieve a circular economy by 2050," https://www.europarl.europa.eu/topics/en/article/20210128STO96607/how-the-eu-wants-to-achieve-a-circular-economy-by-2050.

[12] M. Srivastava and S. Rathee, "Additive manufacturing: recent trends, applications and future outlooks," *Progress in Additive Manufacturing*, vol. 7, no. 2, pp. 261–287, Apr. 2022, https://doi.org/10.1007/s40964-021-00229-8.

[13] D. Y. Koseoglu-Imer *et al.*, "Current challenges and future perspectives for the full circular economy of water in European countries," *Journal of Environmental Management*, vol. 345, Nov. 2023, Art. no. 118627, https://doi.org/10.1016/j.jenvman.2023.118627.

[14] A. D. Dobrzańska-Danikiewicz, B. Siwczyk, A. Bączyk, and A. Romankiewicz, "Mechanical properties of recycled PLA and PETG printed by FDM/FFM method," *Journal of Achievements in Materials and Manufacturing Engineering*, vol. 119, no. 2, pp. 49–59, 2023, https://doi.org/10.5604/01.3001.0053.9490.

[15] D. Rahmatabadi *et al.*, "4D printing and annealing of PETG composites reinforced with short carbon fibers," *Physica Scripta*, vol. 99, no. 5, May 2024, Art. no. 055957, https://doi.org/10.1088/1402-4896/ad3b40.

[16] N. A. Fountas, I. Papantoniou, J. D. Kechagias, D. E. Manolakos, and N. M. Vaxevanidis, "Modeling and optimization of flexural properties of FDM-processed PET-G specimens using RSM and GWO algorithm," *Engineering Failure Analysis*, vol. 138, Aug. 2022, Art. no. 106340, https://doi.org/10.1016/j.engfailanal.2022.106340.

[17] D. Pratap Singh, V. Kumar Dwivedi, and M. Agarwal, "Application of the DoE approach to the fabrication of cast Al2O3-LM6 composite material and evaluation of its mechanical and microstructural properties," *Materials Today: Proceedings*, In Press, Mar. 2023, https://doi.org/10.1016/j.matpr.2023.03.127.

[18] A. Jaisingh Sheoran and H. Kumar, "Fused Deposition modeling process parameters optimization and effect on mechanical properties and part quality: Review and reflection on present research," *Materials Today: Proceedings*, vol. 21, pp. 1659–1672, Jan. 2020, https://doi.org/10.1016/j.matpr.2019.11.296.

[19] L. Kothandaraman and N. K. Balasubramanian, "Optimization of FDM printing parameters for square lattice structures: Improving mechanical characteristics," *Materials Today: Proceedings*, In Press, Apr. 2024, https://doi.org/10.1016/j.matpr.2024.04.033.

[20] D. G. Zisopol, M. Minescu, and D. V. Iacob, "A Study on the Influence of FDM Parameters on the Tensile Behavior of Samples made of PET-G," *Engineering, Technology & Applied Science Research*, vol. 14, no. 2, pp. 13487–13492, Apr. 2024, https://doi.org/10.48084/etasr.6949.

[21] D. G. Zisopol, M. Minescu, and D. V. Iacob, "A Study on the Influence of FDM Parameters on the Tensile Behavior of Samples made of ASA," *Engineering, Technology & Applied Science Research*, vol. 14, no. 4, pp. 15975–15980, Aug. 2024, https://doi.org/10.48084/etasr.8023.

[22] D. V. Iacob, D. G. Zisopol, and M. Minescu, "Technical-Economical Study on the Optimization of FDM Parameters for the Manufacture of PETG and ASA Parts," *Polymers*, vol. 16, no. 16, Jan. 2024, Art. no. 2260, https://doi.org/10.3390/polym16162260.

[23] P. Q. K. Nguyen *et al.*, "Influences of printing parameters on mechanical properties of recycled PET and PETG using fused granular fabrication technique," *Polymer Testing*, vol. 132, Mar. 2024, Art. no. 108390, https://doi.org/10.1016/j.polymertesting.2024.108390.

[24] M. Bremer, L. Janoschek, D. Kaschta, N. Schneider, and M. Wahl, "Influence of plastic recycling—a feasibility study for additive manufacturing using glycol modified polyethylene terephthalate (PETG)," *SN Applied Sciences*, vol. 4, no. 5, Apr. 2022, Art. no. 156, https://doi.org/10.1007/s42452-022-05039-3.

[25] C. O'Driscoll, O. Owodunni, and U. Asghar, "Optimization of 3D printer settings for recycled PET filament using analysis of variance (ANOVA)," *Heliyon*, vol. 10, no. 5, Mar. 2024, Art. no. e26777, https://doi.org/10.1016/j.heliyon.2024.e26777.

[26] "The Proven Solution for 3D Design and Product Development,| SOLIDWORKS," https://www.solidworks.com/proven-solution-3d-design-and-product-development.

[27] "UltiMaker Cura," https://ultimaker.com/software/ultimaker-cura/.

[28] "Anycubic 4Max Pro 2.0 - High Quality Enclosed 3D Printer." https://store.anycubic.com/products/4max-pro-2-0?srsltid=AfmBOoriLOdYzVB8XtMkEspQvUmNZqx6px9GZ2lP-5YVV3XDVAJXl9RW.

[29] ASTM International, *ASTM D638-14: Standard Test Method for Tensile Properties of Plastics*. West Conshohocken, PA, USA: ASTM International.

[30] "Minitab Statistical Software." https://www.minitab.com/en-us/.